Contrast Variation Small-Angle Neutron Scattering Study of the Structure of Block Copolymer Micelles in a Slightly Selective Solvent at Semidilute Concentrations

Jan Skov Pedersen*

Condensed Matter Physics and Chemistry Department, Risø National Laboratory, Roskilde, DK-4000, Denmark

Ian W. Hamley

School of Chemistry, University of Leeds, Leeds, West Yorkshire LS2 9JT, U.K.

Chang Yeol Ryu and Timothy P. Lodge

Department of Chemistry and Department of Chemical Engineering and Materials Science, University of Minnesota, Minneapolis, Minnesota 55455

Received May 12, 1999; Revised Manuscript Received October 20, 1999

ABSTRACT: The structure of micelles of an asymmetric polystyrene−polyisoprene (PS−PI) diblock copolymer has been studied in di-*n*-butyl phthalate (DBP), which is a slightly selective solvent for PS. The polymer has a molecular weight of 11 500 for the fully deuterated *d*-PS block and 48 500 for the PI block. Contrast variation SANS using mixtures of protonated and deuterated solvent and a polymer volume fraction of 18% at 10 °C were performed to get detailed information on the structure of the micelles. An additional contrast was obtained by performing a small-angle X-ray scattering measurement on a sample in protonated DBP. It was found that micelles are formed with an anisometric PI-rich core surrounded by dissolved *d*-PS chains. The data were analyzed using model form factors of micelles with, respectively, cylindrical and ellipsoidal cores. It was necessary to include a term to describe the concentration fluctuations within the swollen PI cores. The particle interference effects originating from the high volume fraction were described by a hard-sphere structure factor. Both models fit the data well, however, a cylindrical model which includes size polydispersity gives the best fit.

1. Introduction

The formation of micelles in a solvent that is selective for one of the blocks is one of the most important and useful properties of block copolymers. For example, micelles formed by block copolymers can solubilize otherwise insoluble substances, they can be used to microscopically "mix" incompatible substances, and they can stabilize colloidal particles or form microemulsions. There has been substantial work on micellization in dilute solutions of block copolymers, and this has been reviewed.[1−5] In contrast, less attention has been devoted to the structure and properties of semidilute or concentrated solutions of block copolymers.[6−13] In this paper we investigate the structure of anisometric micelles formed in nondilute block copolymer solutions, focusing on diblock copolymers in a solvent that is slightly selective for one of the blocks.

Self-assembly in block copolymer melts is the result of microphase separation of the constituent monomers A and B. In dilute solution, micellization can be induced by unfavorable interactions between the solvent molecules (S) and one of the monomers (B). In semidilute and concentrated solutions one may therefore expect a rich phenomenology, such as A−B, A−S, and B−S interactions as well as various entropic terms to contribute to the free energy. For a solvent of the same quality for the A and B monomers, A−B interactions control the behavior in the same way as in the melt, however, qualitative differences from the melt may exist, for example, the scaling of the ordering concentration with chain length.[6] In the opposite situation, when the solvent is strongly selective, i.e., good for the A block and a nonsolvent for the B block, formation of micelles is expected as in dilute solution; however, the intermicellar interaction may lead to a lattice ordering of the micelles. For a "slightly selective" solvent, i.e., a good solvent for block A and close to a theta solvent for block B, small changes in temperature may result in large changes in solution properties, owing to the changes of the relative importance of the B−S interaction with temperature.

Numerous studies of block copolymer micellar structure and interactions, performed by small-angle scattering, have been reported in the literature.[15] Small-angle neutron scattering is particularly well suited for structure determination when one of the blocks of the polymer chain is perdeuterated and the scattering density of the solvent is varied by using protonated and deuterated solvents.[16−22] In most of these contrast variation studies the scattering data have been analyzed by models which assume centrosymmetry of the micelles. Similar models have been used in other recent studies of block copolymer micelles;[23−29] however, for most contrasts these models do not describe the observed scattering at high scattering vectors. Richter et al.[18] included an empirical term for describing the "blob" scattering originating from the dissolved chains in the corona which surrounds the core of the micelles. This scattering contribution is included explicitly in the

* Author for correspondence.

10.1021/ma990740w CCC: $19.00
Published on Web 12/31/1999

models of the type described by Pedersen and Gerstenberg,[30] which are used in the present work.

Recently we reported an extensive series of measurements on polystyrene−polyisoprene (SI) copolymers in the slightly selective solvent di-*n*-butyl phthalate (DBP).[7] The copolymers were an asymmetric SI diblock, with $M_w = 60 \times 10^3$ g/mol and $f_{PS} = 0.17$ by weight, and the matching SIS triblock with $M_w = 120 \times 10^3$ g/mol and the same composition. The solvent is good for polystyrene (PS), but was found to be a theta solvent for PI near 80 °C.[7,8] Solutions with polymer volume fractions, ϕ, near 0.20 were examined by rheology, flow birefringence, small-angle X-ray scattering (SAXS) and small-angle neutron scattering (SANS). The results indicated that below 10 °C, the copolymers formed micelles with PI-rich cores. Interestingly, these micelles were elongated, with fits to model micellar form factors giving an aspect ratio of about 3. Upon increasing temperature, the micelles began to swell as solvent entered the core, leading to substantial intermicellar interactions. This was indicated by, for example, a 2-order-of-magnitude increase in the solution viscosity. The solutions then underwent an abrupt disordering transition near 43° C. As temperature was further increased, the solution viscosity decreased, but did not reach the level associated with a disordered, entangled solution of chains until 60−70 °C; this behavior was attributed to the progressive dissolution of the micelles, with experimental signatures reminiscent of the substantial concentration fluctuations reported for block copolymer melts and solutions.

In a subsequent paper, the micellar ordering in the same system was examined for polymer concentrations spanning the semidilute and concentrated regimes, $0.1 < \phi < 0.4$.[9] For $\phi < 0.2$, the rheological response was liquidlike and SAXS showed that there was no intermicellar order in the liquid. Above a crossover concentration $\phi \approx 0.2$, ordering of micelles was shown by the presence of a structure factor peak. The ordered micellar structure, identified as hexagonal-packed cylinders for $0.2 < \phi < 0.3$, and lamellar for $\phi > 0.3$, persists up to an order−disorder transition $T \approx 40$ °C for the diblock and triblock solutions studied. At higher temperatures, approximately 15 °C above the ODT for the $\phi = 0.2$ solutions, the micelles break up as the polymer chains dissolve into solution. The domain spacing, d, in the ordered solutions obtained from the principal structure factor peak position, shows a crossover at $\phi \approx 0.2$ in agreement with rheology. At high concentrations d was shown to scale as $d \propto \phi^{-1/3}$.[9] This concentration dependence is opposite to that previously observed for block copolymer solutions in neutral solvents,[10−12] due to the solvent selectivity.

In this paper we present a SANS contrast variation study of the micellar structure at 10 °C with a volume fraction $\phi = 0.18$. Micelles of block copolymers with a deuterated PS block (d-PS−PI) were investigated in detail in mixtures of deuterated and protonated DBP. The SANS measurements are supplemented by a SAXS measurement on a sample prepared in protonated DBP. Two models with, respectively, an ellipsoidal core and a cylindrical core of PI surrounded by solvated PS chains were used for interpreting the data. Fits of similar quality were obtained by the two models. For the lowest fractions of d-DBP, the SANS data are dominated by the scattering from the d-PS blocks whereas the scattering from the PI blocks dominates at higher d-DBP fractions. The analytical expressions for the form factors of models with cores with concentration fluctuations and Gaussian coronal chains was based on the expressions presented by Pedersen and Gerstenberg[30,31] for micelles with a spherical core. Detailed information on the size and shape were obtained which essentially confirmed the results of Lodge et al.[7] deduced from their analysis of SAXS data at the same temperature and concentration. In addition, it was found that the core was significantly solvated and the volume fraction of PI in the core was only 30−35%.

2. Experimental Section

Samples and Solutions. A deuterated (d_8)-polystyrene−polyisoprene diblock, custom synthesized by Polymer Source Inc. (Dorval, Canada), was used in the study. The molecular weights and polydispersity determined by the manufacturer using size exclusion chromatography were $M_w(d\text{-PS}) = 11.5 \times 10^3$ g mol^{-1}, $M_w(\text{PI}) = 48.5 \times 10^3$ g mol^{-1}, and $M_w/M_n < 1.15$. The polymer is closely matched to the undeuterated diblock SI-60 used in the previous studies.[7,9] It was dissolved in mixtures of normal DBP (from Aldrich), denoted h-DBP, and a partially deuterated version of this solvent, d-DBP. The partially deuterated DBP was synthesized by the condensation of 1-butanol (d_9) (Cambridge Isotopes) with phthaloyl chloride (Aldrich). Vacuum distillation was used for purifying the phthaloyl chloride prior to use. The alcohol (2.19 g) was dissolved in 20 mL of dry benzene and 1.1 mL of dry pyridine. The mixture was cooled with ice water, under dry nitrogen. The acid chloride (0.73 mL) was added dropwise, and the solution left overnight. A small amount (1.1 g) of (dimethylamino)pyridine was then added, and the reaction allowed to proceed for 3 h. The mixture was worked up with ether and rinsed with 10% aqueous cupric sulfate and water. The product was purified on a silica gel column using 5:1 hexane/ethyl acetate. The synthesized molecule is deuterated at the two butyl chains so that the molecule is deuterated at 18 out of 22 hydrogen positions ($C_6H_4[CO_2(CD_2)_3CD_3]_2$). The DBP was washed with a 5% aqueous solution of $NaHSO_3$ followed by distilled water, dried over $CaCl_2$, and vacuum-distilled prior to use.

The density of protonated DBP is 1.043 g/cm^3 and the neutron scattering length density is $\rho_{DBP} = 1.07 \times 10^{10}$ cm^{-2}. For the deuterated molecule the neutron scattering length density is $\rho_{d-DBP} = 5.30 \times 10^{10}$ cm^{-2}. The mixtures have the solvent scattering neutron length density $\rho_{solv} = x\rho_{d-DBP} + (1 - x)\rho_{DBP}$, where x is the molar fraction of deuterated DBP in the solvent. Mixtures with $x = 0$, 0.28, 0.53, 0.71, and 1 were used in the experiment. The solutions were prepared gravimetrically with volume fractions of polymer of $\phi = 0.18$. For the deuterated polystyrene we used a specific density of 1.12 g/cm^3 and a corresponding neutron scattering length density of $\rho_{d-PS} = 6.50 \times 10^{10}$ cm^{-2}. For the isoprene we used a specific density of 0.91 g/cm^3 and a corresponding neutron scattering length density of $\rho_{PI} = 0.30 \times 10^{10}$ cm^{-2}. The scattering length densities for SAXS are proportional to the electron densities. These are for PS, PI, and DBP, respectively, 0.337, 0.306, and 0.339 e/Å^3. This gives the excess electron densities 0.002 and 0.033 e/Å^3 for PS and PI, respectively.

Small-Angle Neutron and X-ray Scattering. Neutron scattering experiments were conducted at the SANS facility at DR3 at Risø National Laboratory, Denmark.[33] Neutrons with wavelengths 2.8 and 4.7 Å with a resolution $\Delta\lambda/\lambda = 0.18$ (fwhm) were used to cover the scattering vector range $q = 0.0075-0.51$ Å^{-1}. Three combinations of wavelength (λ) and sample-to-detector distance l were used ($\lambda/l = 2.8$ Å/1.1 m, 2.8 Å/3.0 m, and 4.7 Å/6.0 m). The samples were kept in Hellma quartz cells with a path length of 1 or 2 mm depending on the fraction of deuterated solvent. The isotropic two-dimensional scattering spectra were azimuthally averaged to obtain the intensity versus the modulus, q, of the scattering vector, $q = 4\pi \sin\theta/\lambda$, where 2θ is the scattering angle. The data were background subtracted and converted to absolute scale by

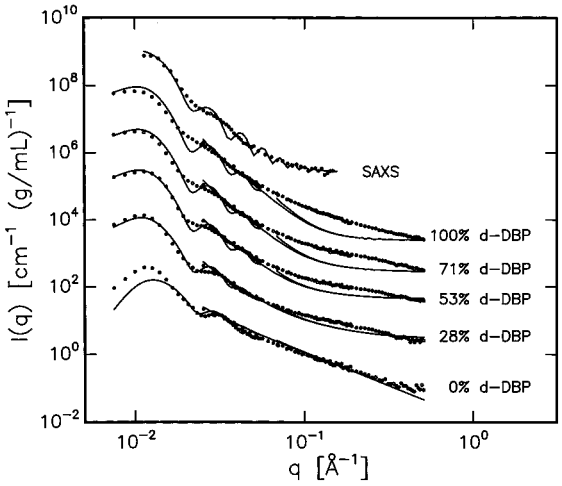

Figure 1. Small-angle scattering data for the contrast variation. From bottom to top the data are the SANS results for 0, 28, 53, 71, and 100% *d*-DBP, respectively. The top data set is the SAXS results. For clarity the 28, 53, 71, and 100% *d*-DBP data has been multiplied by 10, 100, 1000, and 1000, respectively. The curves are the fits obtained for the monodisperse model for micelles with a spherical core without concentration fluctuations. Backgrounds have been adjusted so that the model curves agree with the data at high q. Note that the fitted curves are discontinuous in the overlap region of the data recorded at different instrumental settings due to the smearing with the respective instrumental resolution functions.

dividing by the scattering recorded for pure water in a cell with 1 mm path length. The data were furthermore normalized by the transmission, sample thickness, and polymer concentration.

An X-ray scattering experiment was performed at room temperature on a sample prepared in hydrogenated DBP. The polymer concentration was the same as for the samples used for the SANS. The measurements were done using the pinhole SAXS camera at Risø National Laboratory. The camera uses the Cu $K\alpha$ radiation from a rotating 18 kW Rigaku anode. The radiation is monochromated by a flat graphite pyrolytic crystal, and the beam is collimated by three collinear square slits. The two-dimensional data sets were recorded using an image plate detector. The sample was contained in a glass capillary with a diameter of 2 mm. The sample was transferred to the capillary using a syringe. The SAXS spectrum for this sample was anisotropic, and therefore the sample and capillary were heated and kept for about 10 min at 80 °C. The room temperature SAXS spectrum of this sample was isotropic and the data were azimuthally averaged. The background measured with a capillary filled with pure DBP was subtracted. No attempts were made to convert the SAXS data to absolute scale.

3. Results

Experimental Results. The SANS contrast variation data are shown in Figure 1. The intensity varies by less than a factor of 5 at high scattering vectors (q) whereas it varies by about a factor of 100 at the lowest q. The data show a peak at low q which becomes more pronounced the lower the fraction of deuterated solvent. At high q the data follow approximately a q^{-2} behavior for all contrasts. The SAXS data are also shown in Figure 1. They look quite similar to the data recorded in 100% *d*-DBP, which can be understood from the relative scattering contrasts. For SAXS the contrast of PI is much larger than for PS, and the situation is similar for the SANS in 100% *d*-DBP, for which the contrast of PI is large and that of *d*-PS is very low.

As the solvent is slightly better for PS than for PI, we expect that in agreement with our previous findings[7] the PI will form a micellar core and that the PS will form a diffuse corona of chains surrounding the core. However, there are several different possible structures for such micelles: The most simple morphologies are those with a spherical core, an ellipsoidal core, and a cylindrical core. In our previous study[7] of PS−PI in DBP, we found that the micelles have an ellipsoidal core and the present contrast variation measurements are in agreement with this model. In the analysis of the present data, form factors for micellar models with spherical, elliptical, and cylindrical cores[30,31,34] were used in combination with a hard-sphere structure factor for describing the intermicellar interactions.[32] The expressions for the form factors and the structure factor are summarized in the following.

Model Form Factors and Structure Factor. (i) Form Factor. The form factor of a micelle contains four different terms: the self-correlation of the core, the self-correlation of the chains, the cross-term between the core and chains, and the cross-term between different chains. It can be written[30,34]

$$F_{\mathrm{mic}}(q) = N\beta_{\mathrm{core}}{}^2F_{\mathrm{core}}(q) + N\beta_{\mathrm{chain}}{}^2F_{\mathrm{chain}}(q) + 2N\beta_{\mathrm{core}}\beta_{\mathrm{chain}}S_{\mathrm{core-chain}}(q) + N(N-1)\beta_{\mathrm{chain}}{}^2S_{\mathrm{chain-chain}}(q) \quad (1)$$

where q is the scattering vector, N is the aggregation number of the micelle and β_{core} and β_{chain} are the total excess scattering length of one PI block and one PS block, respectively. The PS chains have a radius of gyration R_g, and the self-correlation term of the Gaussian chains is given by the Debye function:

$$F_{\mathrm{chain}}(q) = \frac{2[\exp(-x) - 1 + x]}{x^2} \quad (2)$$

where $x = q^2R_g{}^2$.

Expressions for $F_{\mathrm{core}}(q)$ and $S_{\mathrm{core-chain}}(q)$ for micelles with spherical cores were given in ref 30. In the following the expressions for ellipsoidal and cylindrical cores are given.

(ii) Ellipsoidal Micelles. For an ellipsoidal core with semiaxes $(R,R,\epsilon R)$, the normalized self-correlation term $[F_{\mathrm{core}}(q = 0) = 1]$ is given by[35]

$$F_{\mathrm{core}}(q) = \int_0^{\pi/2}\Phi^2[q,r(R,\epsilon,\alpha)]\sin\alpha\,\mathrm{d}\alpha \quad (3)$$

where $r(R,\epsilon,\alpha) = R(\sin^2\alpha + \epsilon^2\cos\alpha)^{1/2}$ and

$$\Phi(q,r) = \frac{3[\sin(qr) - qr\cos(qr)]}{(qr)^3} \quad (4)$$

In the following the short notation $r = r(R,\epsilon,\alpha)$ will be used for convenience. The interference cross-term between the core and Gaussian chains starting at d away from the surface of the core is

$$S_{\mathrm{core-chain}}(q) = \psi(q,R_g)\int_0^{\pi/2}\Phi(q,r)\frac{\sin(q[r+d])}{q[r+d]}\sin\alpha\,\mathrm{d}\alpha \quad (5)$$

The function $\psi(q,R_g) = [1 - \exp(-x)]/x$ is the form factor amplitude of the chain.[37] Finally, the interference

term between the chains is

$$S_{\text{chain-chain}}(q) = \psi^2(q,R_g)\int_0^{\pi/2}\left[\frac{\sin(q[r+d])}{q[r+d]}\right]^2 \sin\alpha\, d\alpha \quad (6)$$

The fitting showed that a model for a micelle with a spherical core was not able to fit the full set of contrast variation data (see Figure 1 and the discussion in the next section). The main deviations for the scattering intensity were found for the 100% *d*-DBP where the *d*-PS is almost matched and the scattering is dominated by the PI core. The model gives a q^{-4} behavior in this region whereas the data follow a q^{-2} behavior. This deviation can be explained by scattering from concentration fluctuations in the core due to swelling by the solvent. This will give rise to a scattering signal which is similar to the scattering from a semidilute polymer solution. For the present swollen micelles the scattering from the concentration fluctuations is so significant that they need to be incorporated into the model.

We take the concentration fluctuations to have a correlation length ξ and describe them as a collection of n_{blob} independent blobs with radius of gyration $R_g^{\text{blob}} = \xi\sqrt{3}$. The scattering from a blob is expected to be reasonably well described by a Lorentzian of the form $1/[1 + (\xi q)^2]$; however, to be able to calculate the form factor analytically, we use the Debye function for a Gaussian polymer instead. The number of blobs in the core is approximately $n_{\text{blob}} = V_{\text{core}}/V_{\text{blob}}$, where V_{core} is the volume of the core and V_{blob} is the volume of one blob which can be estimated as $V_{\text{blob}} = 4\pi(R_g^{\text{blob}})^3/3$. The number of blobs is only roughly estimated, and to allow for adjustments, we use $n_{\text{blob}} = A_1 V_{\text{core}}/V_{\text{blob}}$, where A_1 is a fitting parameter.

The blobs are uniformly distributed over the core, and therefore the core term in (1) is replaced by a blob−blob term and a blob self-correlation term. This gives

$$F_{\text{core}}(q) = [n_{\text{blob}}(n_{\text{blob}} - 1)\psi^2(q,R_g^{\text{blob}}) \times \int_0^{\pi/2}\Phi^2(q,r)\sin\alpha\, d\alpha + n_{\text{blob}}F_{\text{chain}}(q,R_g^{\text{blob}})]/n_{\text{blob}}^2 \quad (7)$$

The chain self-correlation term and the chain−chain correlation term are unaltered, whereas the core−chain term becomes

$$S_{\text{core-chain}}(q) = \psi(q,R_g)\,\psi(q,R_g^{\text{blob}}) \times \int_0^{\pi/2}\Phi^2(q,r)\frac{\sin[q(d+r)]}{q(d+r)}\sin\alpha\, d\alpha \quad (8)$$

(iii) Cylindrical Micelles. For a cylindrical core with radius R and length L, the normalized self-correlation term is[36]

$$F_{\text{core}}(q,R,L) = \int_0^{\pi/2}\Psi(q,R,L,\alpha)^2\sin\alpha\, d\alpha \quad (9)$$

where

$$\Psi(q,R,L,\alpha) = \frac{2B_1(qR\sin\alpha)}{qR\sin\alpha}\frac{\sin(qL\cos\alpha/2)}{qL\,\alpha/2} \quad (10)$$

and $B_1(x)$ is the first-order Bessel function of the first kind.

The interference cross-term between the core and Gaussian chains starting at d away from the surface of the core, i.e., on a coaxial cylindrical shell with radius $R + d$ and length $L + 2d$, is (Note that there are errors in the expressions given in ref 34.)

$$S_{\text{core-chain}}(q) = \psi(q,R_g)\int_0^{\pi/2}\Psi(q,R,L,\alpha) \times \Xi(q,R+d,L+2d,\alpha)\sin\alpha\, d\alpha \quad (11)$$

where

$$\Xi(q,R,L,\alpha) = \left[\frac{R}{(R+L)}\frac{2B_1(qR\sin\alpha)}{qR\sin\alpha} \times \cos(qL\cos\alpha/2) + \frac{L}{(R+L)} \times B_0(qR\sin\alpha)\frac{\sin(qL\cos\alpha/2)}{qL\cos\alpha/2}\right] \quad (12)$$

In this equation $B_0(x)$ is the zero-order Bessel function of the first kind. The interference term between the chains is

$$S_{\text{chain-chain}}(q) = \psi^2(q,R_g) \times \int_0^{\pi/2}\Xi(q,R+d,L+2d,\alpha)^2\sin\alpha\, d\alpha \quad (13)$$

Including the scattering from blobs in the core modifies the core self-correlation term to

$$F_{\text{core}}(q) = [n_{\text{blob}}(n_{\text{blob}} - 1)\psi^2(q,R_g^{\text{blob}}) + \int_0^{\pi/2}\Psi^2(q,R,L,\alpha)\sin\alpha\, d\alpha + n_{\text{blob}}F_{\text{chain}}(q,R_g^{\text{blob}})]/n_{\text{blob}}^2 \quad (14)$$

The chain self-correlation term and the chain−chain correlation term are again unaltered, whereas the core−chain term becomes

$$S_{\text{core-chain}}(q) = \psi(q,R_g)\,\psi(q,R_g^{\text{blob}}) \times \int_0^{\pi/2}\Psi(q,R,L,\alpha)\,\Xi(q,R+d,L+2d,\alpha)\sin\alpha\, d\alpha \quad (15)$$

The total neutron scattering lengths which enter (1) are $\beta_{\text{core}} = V_{d-\text{PS}}(\rho_{d-\text{PS}} - \rho_{\text{solv}})$ and $\beta_{\text{chain}} = V_{\text{PI}}(\rho_{\text{PI}} - \rho_{\text{solv}})$, where $V_{d-\text{PS}} = 1.71 \times 10^{-20}$ cm^3 and $V_{\text{PI}} = 9.12 \times 10^{-20}$ cm^3. The relative total SAXS scattering lengths are calculated similarly from the excess electron densities, where excess means in excess of the electron density of the solvent. The total numbers of excess electrons are 34.1 for PS and 3010 for PI. We want to allow the presence of solvent in the core, and therefore the volume of the core is given by $V_{\text{core}} = NV_{\text{PI}}/(1 - f)$, where f is the volume fraction of solvent in the core.

Structure Factor. The volume fraction of the micelles is so large that their interaction has to be included in the analysis. This is done using the structure factor of a monodisperse hard-sphere liquid[38,39] combined with an approximation similar to the decoupling approximation.[40] The hard-sphere structure factor has previously been shown to give a good description of the structure factor of spherical micelles.[23] For the micelles with Gaussian chains on the surface the intensity is given by[32]

$$I(q) = F_{\text{mic}}(q) + A_{\text{mic}}(q)^2[S(q) - 1] \quad (16)$$

where $S(q)$ is the monodisperse hard-sphere structure factor and $A_{\text{mic}}(q)$ is the form factor amplitude of the

radial scattering length distribution of the micelle.[32] For ellipsoidal micelles it is

$$A_{\mathrm{mic}}(q) = \beta_{\mathrm{core}}\psi(q,R_{\mathrm{g}}^{\mathrm{blob}}) \int_0^{\pi/2} \Phi(q,r) \sin\alpha \, \mathrm{d}\alpha + \beta_{\mathrm{chain}}\psi(q,R_{\mathrm{g}}) \int_0^{\pi/2} \frac{\sin[q(r+d)]}{q(r+d)} \sin\alpha \, \mathrm{d}\alpha \quad (17)$$

For cylindrical micelles it is given by

$$A_{\mathrm{mic}}(q) = \beta_{\mathrm{core}}\psi(q,R_{\mathrm{g}}^{\mathrm{blob}}) \int_0^{\pi/2} \Psi(q,R,L,\alpha) \sin\alpha \, \mathrm{d}\alpha + \beta_{\mathrm{chain}}\psi(q,R_{\mathrm{g}}) \int_0^{\pi/2} \Xi(q,R+d,L+2d,\alpha) \sin\alpha \, \mathrm{d}\alpha \quad (18)$$

We note that for micelles with an ellipsoidal or a cylindrical core eq 16 is a rather crude approximation owing to the assumption of centrosymmetric interactions. However, more reliable expressions are to our knowledge not available for particles with a relatively modest anisotropy (see the results below). The structure factor $S(q)$ entering eq 16 depends on two parameters, the hard-sphere interaction radius R_{hs} and the hard-sphere volume fraction η. These parameters were allowed to vary freely in the fits, and as a consequence of the anisotropy of the particles, the resulting values should only be considered as effective values.

The scattering cross section for the model in absolute units for data normalized by the concentration is given by

$$\frac{\mathrm{d}\sigma(q)}{\mathrm{d}\Omega} = \frac{I(q)}{\rho_{\mathrm{p}} N V_{\mathrm{p}}} \quad (19)$$

where $I(q)$ is given by eq 16, ρ_{p} is the specific density of the block copolymer, N is the aggregation number, and V_{p} is the volume of one polymer chain.

When the model is fitted to the experimental data, the model scattering intensity (eq 16) is smeared by the finite instrumental resolution.[41] For each setting the intensity is convoluted with the appropriate resolution function. Note that all five SANS contrast variation data sets and the SAXS data were fitted simultaneously, with one structural model in which the contrast of the core and the contrast of the chains were varied appropriately.

The fitting parameters of the models are aggregation number N, eccentricity ϵ for ellipsoidal micelles or the length L for cylindrical micelles, solvent volume fraction in the core f, radius of gyration of the PS chains R_{g}, displacement of the chains d, equivalent radius of gyration of the concentration fluctuations in the core $R_{\mathrm{g}}^{\mathrm{blob}}$, scale factor for fluctuation contribution A_1, effective hard-sphere volume fraction η, and effective hard-sphere interaction radius R_{hs}. An overall scale factor was also used for fitting the SAXS data which are on an arbitrary scale. This gives seven parameters for describing the micellar structure and two parameters for describing the interactions.

Fit Results. The first models that were fitted to the data were the models for micelles with a spherical core (i.e., with $\epsilon = 1$ for the models with ellipsoidal cores). Without the concentration fluctuations in the core (Figure 1), the model gives a rather poor fit to the data at high q except for the 0% *d*-DBP data. Note that the curves are discontinuous in the overlap regions of the data from the 1, 3, and 6 m setting, due to the smearing with the resolution function which is different for each setting. The agreement of the model with the data is significantly improved by the inclusion of the fluctuations (Figure 2); however, the model gives too pronounced form factor oscillations except for the 0% *d*-DBP data. Including polydispersity of the aggregation number for micelles with a spherical core improves the fit further (Figure 3); however, for this model the form factor oscillations are too smeared for the 0% *d*-DBP data. A fit with a model with ellipsoidal cores is quite satisfactory with the main deviations in the region of the peak for the 0% *d*-DBP data (Figure 4). When the data were fitted by the ellipsoidal model the hard-sphere volume fraction tended to be larger than 0.5, which is the threshold value for freezing or "jamming" of a hard-sphere liquid. As this was not considered reasonable, the value was in this case fixed at $\eta = 0.50$. We note that the influence of the value of η on the other parameters is relatively small for values close to 0.5.

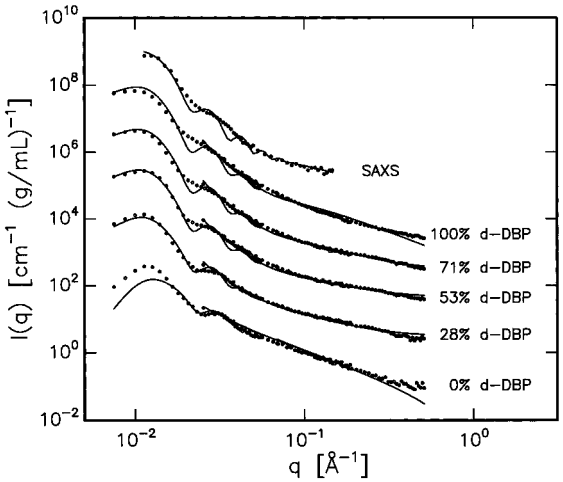

Figure 2. The same small-angle scattering data as in Figure 1. The curves are the fits obtained for a monodisperse model for micelles with a spherical core with concentration fluctuations.

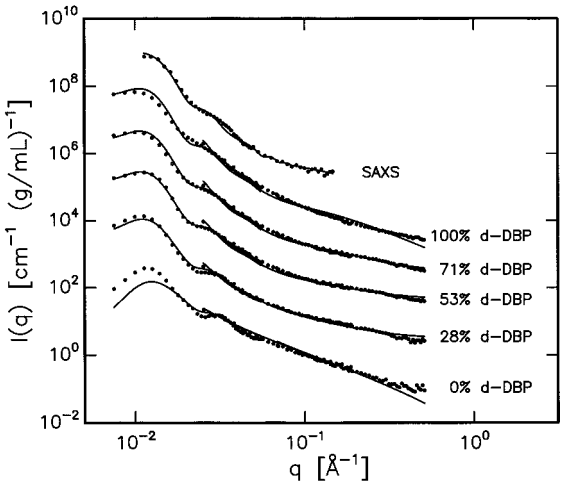

Figure 3. The same small-angle scattering data as in Figure 1. The curves are the fits obtained for a polydisperse model for micelles with a spherical core with concentration fluctuations.

The results for the parameters from the fit of the ellipsoidal model are given in Table 1, and these show that the micelles are significantly elongated with a quite high fraction of solvent in the core. Also given in the table are the values obtained by Lodge et al.[7] for small-angle X-ray scattering data analyzed by a similar model without fluctuations in the core. The results agree very

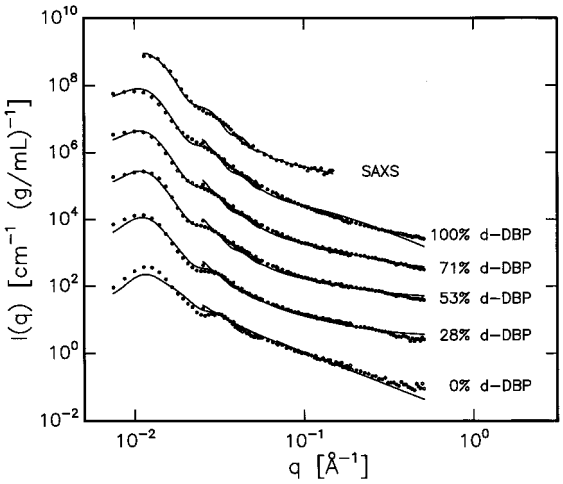

Figure 4. The same small-angle scattering data as in Figure 1. The curves are the fits obtained for a monodisperse model for micelles with an ellipsoidal core with concentration fluctuations.

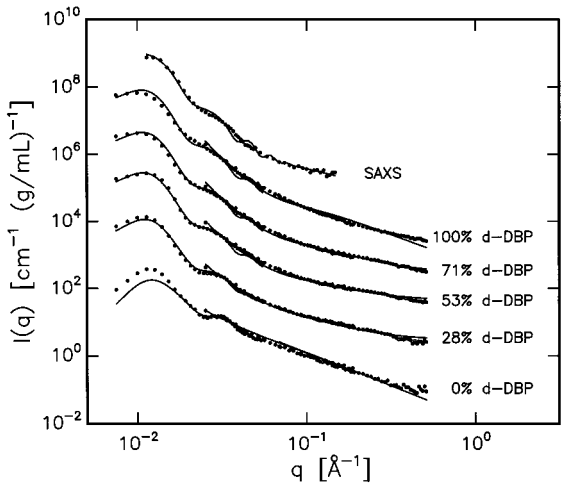

Figure 5. The same small-angle scattering data as in Figure 1. The curves are the fits obtained for a monodisperse model for micelles with a cylindrical core with concentration fluctuations.

Table 1. Results for the Ellipsoidal and the Cylindrical Model[a]

parameter	SANS ellipsoidal	SANS cylindrical	SANS polyd. cylin.	SAXS ellipsoidal
N	370	180	310[b]	(940) 330
ϵ	2.5	–	–	2.7
L (Å)	–	470	715[c]	
f	0.65	0.70	0.65	–
R_g (Å)	43	39	40	32
d/R_g	0.45	0.80	0.61	0.14
R_g^{blob} (Å)	14	15	14	–
A_1	2.0	2.1	2.0	–
η	0.50[d]	0.37	0.50[d]	–
R_{hs} (Å)	310	280	305	–
R (Å) (calcd)	210	190	205[e]	200
Σ (Å^2) (calcd)	3120	4380	3820	–
s (Å^2) (calcd)	5810	4780	5030	–
s/Σ (calcd)	1.9	1.1	1.3	–

[a] The SANS columns refer to the contrast variation SANS data in the present work and the model with concentration fluctuations in the core. The SAXS column refers to the result of Lodge et al.[7] for small-angle X-ray scattering data. [b] The weight-averaged value ($\langle N^2\rangle/\langle N\rangle$) is given. [c] The intensity-averaged value ($\langle L^2V^2\rangle/\langle V^2\rangle^{1/2}$) is given. [d] Fixed for the final fit. [e] The intensity-averaged value ($\langle R^2V^2\rangle/\langle V^2\rangle^{1/2}$) is given.

well. The aggregation number is 370 for the SANS model and 940 for the SAXS model; however, the analysis of the SAXS data was not done on an absolute scale and it was therefore not possible to determine the fraction of solvent in the core. Using the value of $f = 0.65$ from the SANS data, we obtain an aggregation number of 330 for the SAXS data.

For the present data the radius of gyration R_g of the PS chains is determined to be 43 Å, which is somewhat larger than the unperturbed value of 30 Å for a polystyrene chain with the same molecular mass.[43,44] The size of the PS chains may indicate brushlike chains;[45] however, as discussed below, the surface density of chains suggests weakly interacting chains and thus mushroom polymer configurations.[45] The displacement of the chains relative to the core surface is less than R_g, which is the value expected from Monte Carlo simulations.[30] This might suggest some mixing of PS and PI at the interface between core and corona.

The radius of gyration of the concentration fluctuations in the core R_g^{blob} corresponds to a correlation length $\xi = 7.7$ Å. This is in excellent agreement with the value of 7.3 Å for hydrogenated polybutadiene at a concentration of 35%[46] and is somewhat larger than the value of 5.5 Å for a 35% solution of PS in toluene, which can be calculated from the expressions in ref 47.

The short (R) and long (ϵR) half axes of the core can be calculated from the aggregation number, the solvent fraction in the core, and the volume of a PI block. They are, respectively, 210 and 525 Å, whereas the effective hard-sphere radius is 310 Å. One should note that the chains extend approximately $2R_g = 86$ Å further than the core radius and therefore the hard-sphere radius should be compared to $R_{core} + 2R_g$ and $\epsilon R_{core} + 2R_g$, which are 300 and 610 Å, respectively. The value of R_{hs} is close to the lowest value, suggesting that the intermicellar correlations are dominated by local parallel packing arrangements of the micelles. The effective hard-sphere volume fraction of the micelles was fixed at $\eta = 0.5$, which is much larger than the volume fraction of the polymer, $\phi = 0.18$. However, it should be kept in mind that the cores are significantly swollen and that the corona of PS chains extends far into the solvent. The volume fraction of the swollen PI cores is about $\phi_{core} = 0.42$, which is already close to the effective value determined.

The next model that was fitted to the data was the one for micelles with cylindrical cores (Figure 5). The overall agreement as measured by χ^2 [42] is better than for the ellipsoidal model; however, the model fits the 0% DBP worse at low q in the peak region than the model with ellipsoidal cores. Some deviations are also present for the SAXS data, for which the model gives too pronounced form factor oscillations. The results for the parameters are given in Table 1. The length is much smaller than the length from the ellipsoidal model ($2\epsilon R$), whereas the radius is similar. The cylindrical model also gives similar results for solvent fraction, fluctuation correlation length, and radius of gyration of the PS chains and their displacement. The effective hard-sphere volume fraction and hard-sphere radius are significantly smaller than for the ellipsoidal model.

The model that gave the best fit to the data is a cylindrical model with polydispersity of the aggregation number (Figure 6). It should be noted that a similar polydisperse model for micelles with an ellipsoidal core resulted in a fit that was only slightly better than obtained by the corresponding monodisperse model.

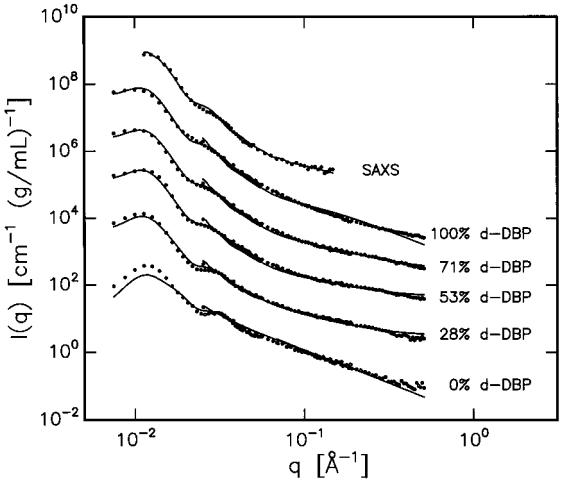

Figure 6. The same small-angle scattering data as in Figure 1. The curves are the fits obtained for a polydisperse model for micelles with cylindrical cores with concentration fluctuations.

For the cylindrical model, a Gaussian distribution of aggregation numbers was assumed:

$$D(N) = \exp[-(N - \langle N\rangle)^2/{\sigma_N}^2]/(\sqrt{2\pi}\sigma_N) \qquad (20)$$

In this expression $\langle N\rangle$ is the average aggregation number and σ_N is the width of the distribution, which is truncated at $N = 0$. The micelles are assumed to have the same solvent fraction in the core, the same aspect ratio $L/(2R)$, the same R_g of the PS, chains and the same displacement d.

The scattering cross section of the model in absolute units for data normalized by the polymer concentration is

$$\frac{d\sigma(q)}{d\Omega} = \frac{1}{\rho_p V_p}\frac{\langle I(q)\rangle}{\langle N\rangle} \qquad (21)$$

in which $\langle\cdot\rangle$ means average with respect to the distribution $D(N)$. For a parameter $P(N)$, it is given by

$$\langle P\rangle = \int_0^\infty P(N)\, D(N)\, dN \qquad (22)$$

The fits obtained by the polydisperse model are shown in Figure 6. The fits to the data are quite satisfactory; however, as for the other models some deviations in the region of the peak for the 0% *d*-DBP data are observed. The results for the fits are given in Table 1. For the aggregation number, the length, and the radius, values weighted as in the scattering experiment are given, i.e., weight-averaged value $N_w = \langle N^2\rangle/\langle N\rangle$ for the aggregation number and intensity-averaged (*z*-averaged) values, $L_I = (\langle L^2N^2\rangle/\langle N^2\rangle)^{1/2}$ and $R_I = (\langle R^2N^2\rangle/\langle N^2\rangle)^{1/2}$, for length and radius, respectively.

The values of the parameters for the polydisperse cylindrical model (Table 1) are quite similar to those obtained for the ellipsoidal model, except that the aggregation number is about 20% smaller. The aspect ratio of the cylindrical core is $L/(2R) = 1.7$, which is also smaller than the eccentricity $\epsilon = 2.5$ of the ellipsoidal micelles. The effective hard-sphere volume fraction tended to be larger than 0.5, and it was therefore fixed at this value during the final fit. The polydispersity of the aggregation number is $\sigma(N)/N = 0.40$ with a corresponding polydispersity of the radius and of the length of $\sigma(R)/R = \sigma(L)/L = 0.13$.

The importance of the interactions between the PS chain on the surface can be investigated by comparing the surface area Σ available for each chain to the size of a chain estimated as $s = \pi {R_g}^2$. The available surface area per chain is $\Sigma = 2\pi R^2[1 + \arcsin(e)/e]/N$ for the ellipsoidal cores, and $\Sigma = 2\pi R(R + L)/N$ for the cylindrical cores, where $e = (1 - \epsilon^{-2})^{1/2}$. The values for Σ and s are given in Table 1 together with the ratio s/Σ, which can be considered as the surface concentration of chains relative to an overlap concentration. The ratio s/Σ is 1.1−1.6 for the three fitted models, which means that the interaction between chains is weak. This suggests mushroom polymer configurations in the corona. For comparison the same quantity is about 2.5 for micelles of poly(ethylene oxide)−poly(propylene oxide)−poly(ethylene oxide) ($EO_{25}PO_{40}EO_{25}$) in water at 50 °C[48] and about 10 for micelles of poly(ethylene oxide)−poly(butylene oxide) ($EO_{90}BO_{10}$) in water also at 50 °C.[49] Of the values available, the micelles of PS−PI in DBP are those with the weakest interchain interactions. One may note that the polymer in this case is the one with the smallest solvophilic block. The $EO_{25}PO_{40}EO_{25}$ polymer is close to symmetric with 25 EO monomers for each 20 PO monomers, whereas $EO_{90}BO_{10}$ is the polymer with the longest solvophilic part relative to the solvophobic part. Therefore, the available values for s/Σ might suggest that the importance of interchain interactions increases with the relative length of the solvophilic block. However, it might also be because the solvent quality for the coronal chains differs.

It is also interesting to compare the available surface area per chain Σ for the three systems. It is about 4000 Å^2 for the PS−PI/DBP system, about 220 Å^2 for the $EO_{25}PO_{40}EO_{25}$/water system, and about 250 Å^2 for the $EO_{90}BO_{10}$/water system. The two latter systems are those with the most solvophobic core blocks, and Σ is similar for these and a factor of 16−18 lower than for the less solvophobic PS−PI/DBP system. The degree of solvophobicity is also reflected in the solvent content of the cores in these three system. It is 65% for PS−PI/DBP, 30% for $EO_{25}PO_{40}EO_{25}$/water and 30−50% for $EO_{90}BO_{10}$/water. In principle the BO is the most solvophobic; however, the confinement of the EO chains and their strong interaction cost configurational entropy, which prevents a close packing of the BO blocks in the core.

Cross-Section Profile. The cross-section structure of the micelles can be calculated as the Fourier transform of the "radial" part (eq 17) of the form factor.[32] To obtain the structure of the ellipsoid micelle along one of the short axes, it has to be placed in a Cartesian coordinate system with an origin coinciding with the center of the micelle, the x and y axes lying along the two short axes, and the z axis lying along the long axis. The amplitude is then

$$A_{mic}{}^V(q_x,q_y,q_z) = V_{PI}\psi(q,R_g{}^{blob})\,\Phi(q,[R^2({q_x}^2 + {q_y}^2) + \epsilon^2R^2{q_z}^2]) + V_{PS}\psi(q,R_g) \times \frac{\sin([(R+d)^2({q_x}^2+{q_y}^2) + (\epsilon R + d)^2{q_z}^2])}{[(R+d)^2({q_x}^2+{q_y}^2) + (\epsilon R + d)^2{q_z}^2]} \qquad (23)$$

where q_x, q_y, and q_z are the components of the scattering vector along the x, y, and z axes, respectively. In the equation, the total scattering lengths have been replaced

by the volumes V_{PI}, the total volume of the PI chains, and V_{PS}, the total volume of the PS chains. As a result of this, the function obtained by Fourier transformation is proportional to the volume fraction distribution. It is straightforward to normalize it, by ensuring that it gives the correct volume fraction of PI in the core. For the same normalization, the distribution of the PI and of the PS can be obtained separately by setting $V_{PS} = 0$ or $V_{PI} = 0$ in the amplitude, respectively.

The function for $y = 0$ and $z = 0$ along x is obtained by integrating over q_y and q_z. Note that the Gaussian statistics of the chains in the model persists down to infinitesimal distances, which is, of course, unphysical. Therefore the amplitude was multiplied by the cutoff function $\exp(-q^2R_0^2/8)$, where $R_0 = 4.5$ Å is similar to the typical dimension of a styrene monomer. Note that $\exp(-q^2R_0^2/4)$ is the cross-section Guinier expression for cylinders with a cross-section radius R_0 and that it is the square root of this function which is used for the amplitude.

The volume fraction distribution in the radial direction is given by

$$\rho(x) = C \int_0^\infty A_{mic}{}^V(q_x,q_y,q_z) \cos(q_x x)\, dq_x\, dq_y\, dq_z \quad (24)$$

where C is determined from the normalization, where the fact that the integrand is symmetric with respect to x has been used. In practice the integration is carried out numerically.

The radial profile of cylindrical micelles can be obtained by a similar approach. It is much easier due to the cylindrical symmetry and the fact that the amplitude is factorized so that the z integration can be done analytically. The volume fraction distribution in the radial direction is given by the (zero order) Bessel function transform of

$$A_{mic}{}^V(q) = V_{PS}\psi(q,R_g{}^{blob})\frac{2B_1(qR)}{qR} + V_{PI}\psi(q,R_g)\, B_0(qR) \quad (25)$$

The radial volume fraction distributions of the polymers were calculated for the best fits of the ellipsoidal and cylindrical models using the expressions given above (eqs 23−25). The profiles are quite similar, and therefore only the profile for the cylindrical model (Figure 7) is discussed.

The surface of the PI core is smooth due to the fluctuations in the core. The PS chains have a well-defined distribution at the surface of the core with some smaller overlap with the PI chains in the core. The maximum volume fraction of the PS corona is less than about 7% compared to the 35% of the PI core. The PS corona is relatively narrow and can be considered simply to "coat" the swollen PI cores.

4. Summary and Conclusions

Contrast variation SANS measurements supplemented by a SAXS measurement have been performed on a *d*-PS−PI block copolymer in DBP with a volume fraction of 18%. Models for the form factor showed that a micelle with an ellipsoidal or cylindrical PI core surrounded by solvated Gaussian PS chains could fit the data. To obtain a satisfactory fit, it was necessary to include concentration fluctuations in the core.

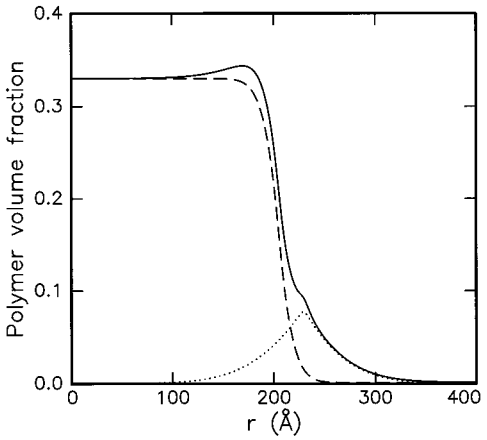

Figure 7. Cross-section volume fraction of the cylindrical micelles along radius. The structure is given as volume fractions of, respectively, PS (dotted curve), PI (broken curve), and total (full curve) polymer in the micelle.

To test the significance of the anisometry of the micelles, models with spherical cores were also fitted to the data. Such a model even allowing for fluctuations in the core gave a worse fit than those for anisometric micelles, showing that this model is inadequate. Including polydispersity of the spherical core improved the fit; however, it was still much worse than for the models with elliptical or cylindrical cores. Thus it can be concluded that the anisometry of the micelles is significant. This is in agreement with previous SANS experiments under shear and optical flow birefringence measurements under shear[7] which together demonstrated the presence of anisometric micelles. It is also in agreement with the findings of Bragg reflections from a hexagonal lattice by SAXS for volume fractions $\phi = 0.2-0.33$,[9] which demonstrates parallel ordering of rods.

The models that give good fits to the present contrast variation data differ somewhat in the details, but the qualitative conclusion is that the micelles are elongated with swollen PI cores surrounded by a corona of dissolved PS chains. In general, the fits to the 0% *d*-DBP data are worse than for the other contrasts. The 0% data are close to the overall match point of the polymer, and therefore the fits to these data are particularly sensitive to the composition of the polymer and the solvent, as well as to the combination of form factors and structure factors in the expressions for analyzing the data.[50] The possibility of having a dependence of micellar aggregation on the isotopic composition of the solvent should also be kept in mind, although we have found no conclusive evidence of this in the present study.

The quantitative modeling indicates that the core radius is $R \approx 200$ Å, the core solvent fraction $f \approx 0.7$, and the radius of gyration of the PS chains is $R_g \approx 40$ Å. The determination of the length of the micelles is more uncertain as there are strong intermicellar interaction effects that influence the data in the range of scattering vectors from which the length is determined. The structure factor used for describing the interaction effects is far from perfect as the micelles are anisometric while the structure factor is based on the assumption of centrosymmetric interactions between the micelles. The fact that the micelles can order as rods on a hexagonal lattice at slightly larger volume fraction makes it relevant to consider the possibility that the micelles at $\phi = 0.18$ are long and disordered and form an entangled network of straight or semiflexible rods

with a structure similar to that of a solution of semidilute or concentrated polymer chains. For this purpose, let us first consider the volume fraction of the micelles determined in the present work. The volume fraction of the PI chains is 15%, and with a solvent fraction of 65%, this gives a core volume fraction of 42%. For the cylindrical micelles, neglecting end effects, the total volume fraction of the micelles also includes the PS corona. This procedure gives a volume fraction larger by a factor of $(R + [1 + d]R_g)^2/R^2$, which results in a total micelle volume fraction of 75% which is approaching the value of 91% for hexagonally packed rods. The estimated volume fraction is in good agreement with the observation of hexagonally order rods for $\phi \approx 0.2$, so it is possible that the sample consists of an entangled network of rodlike or semiflexible micelles. The relevant question is then whether such a network can give rise to a structure factor peak such as the one observed. Recent unpublished Monte Carlo simulation results by Pedersen and Schurtenberger[51] on solutions of semiflexible polymer chains interacting with a hard-sphere potential have shown that a structure factor peak is present for volume fractions larger than 20% and that its position is related to the chain−chain distance. Therefore, a structure factor peak is present for entangled chains at high concentration, and for this reason as well it is possible that the micelles are much longer than the values suggested by the modeling in the present work. The simulation results of Pedersen and Schurtenberger[51] at high concentration are not extensive enough to allow a numerical parametrization so that the results can be used for fitting of the present experimental data.

Acknowledgment. The neutron scattering experiments reported in this paper were performed at the DR3 reactor at Risø National Laboratory and supported by the Commission of the European Community through the Training and Mobility of Researchers Programme (TMR). I.W.H. and T.P.L. are grateful to NATO for a Collaborative Research Grant (CRG/940078). I.W.H. acknowledges the support of the Engineering and Physical Sciences Research Council (U.K.). This work was supported in part by the National Science Foundation through Awards DMR-9018807 and DMR-9528481 to T.P.L.

References and Notes

(1) Hamley, I. W. *The Physics of Block Copolymers*; Oxford University Press: Oxford, 1998.
(2) Tuzar, Z.; Kratochvil, P. In *Surface and Colloid Science*; Matijevic, E., Ed.; Plenum Press: New York, 1993; Vol. 15.
(3) Brown, R. A.; Masters, A. J.; Price, C.; Yuan, X. F. In *Comprehensive Polymer Science*; Booth, C., Price, C., Eds.; Pergamon: Oxford, 1989; Vol. 2.
(4) Riess, G.; Hurtrez, G.; Bahadur, P. In *Encyclopedia of Polymer Science and Engineering*; Mark, H. F., Kroschwitz, J. I., Eds.; Wiley: New York, 1985; Vol. 2.
(5) Price, C. In *Developments in Block Copolymers*; Goodman, I., Ed.; Applied Science: London, 1982; Vol. 1.
(6) Lodge, T. P.; Pan, C.; Jin, X.; Liu, Z.; Zhao, J.; Maurer, W. W.; Bates, F. S. *J. Polym. Sci., Polym. Phys. Ed.* **1995**, *33*, 2289.
(7) Lodge, T. P.; Xu, X.; Ryu, C. Y.; Hamley, I. W.; Fairclough, J. P. A.; Ryan, A. J.; Pedersen, J. S. *Macromolecules* **1996**, *29*, 5955.
(8) Ryu, C. Y. Ph.D. Thesis, University of Minnesota, 1998.
(9) Hamley, I. W.; Fairclough, J. P. A.; Ryan, A. J.; Ryu, C. Y.; Lodge, T. P.; Gleeson, A. J.; Pedersen, J. S. *Macromolecules* **1998**, *31*, 1188.
(10) Hashimoto, T.; Shibayama, M.; Kawai, H. *Macromolecules* **1983**, *16*, 1093.
(11) Shibayama, M.; Hashimoto, T.; Hasegawa, H.; Kawai, H. *Macromolecules* **1983**, *16*, 1427.
(12) Mayes, A. M.; Barker, J. G.; Russell, T. P. *J. Chem. Phys.* **1994**, *101*, 5213.
(13) McConnell, G. A.; Gast, A. P. *Phys. Rev. E* **1996**, *54*, 5447.
(14) Raspaud, E.; Lairez, D.; Adam, M.; Carton, J.-P. *Macromolecules* **1994**, *27*, 2956.
(15) Mortensen, K. *J. Phys.: Condens. Matter* **1996**, *8*, A103.
(16) McConnell, G. A.; Lin, E. K.; Gast, A. P.; Huang, J. S.; Lin, M. Y.; Smith, S. D. *Faraday Discuss.* **1994**, *98*, 121.
(17) Iatrou, H.; Willner, L.; Hadjichristidis, N.; Halperin, A.; Richter, D. *Macromolecules* **1996**, *29*, 582.
(18) Richter, D.; Schneiders, D.; Monkenbusch, M.; Willner, L.; Fetters, L. J.; Huang, J. S.; Lin, M.; Mortensen, K.; Farago, B. *Macromolecules* **1997**, *30*, 1053.
(19) Ramzi, A.; Prager, M.; Richter, D.; Efstratiadis, V.; Hadjichristidis, N.; Young, R. N.; Allgaier, J. B. *Macromolecules* **1997**, *30*, 7171.
(20) Poppe, A.; Willner, L.; Allgaier, J.; Stellbrink, J.; Richter, D. *Macromolecules* **1997**, *30*, 7462.
(21) Nakano, M.; Matsuoka, H.; Yamaoka, H.; Poppe, A.; Richter, D. *Macromolecules* **1999**, *32*, 697.
(22) Goldmint, I.; Yu, G.-E.; Booth, C.; Smith, K. A.; Hatton, T. A. *Langmuir* **1999**, *15*, 1651.
(23) Mortensen, K.; Pedersen, J. S. *Macromolecules* **1993**, *26*, 805.
(24) Chu, B.; Wu, G.; Schneider, D. K. *J. Polym. Sci.: Part B* **1994**, *32*, 2605.
(25) Liu, Y.; Chen, S.-H.; Huang, J. S. *Macromolecules* **1998**, *31*, 2236.
(26) Goldmint, I.; von Gottberg, F. K.; Smith, K. A.; Hatton, T. A. *Langmuir* **1997**, *13*, 3659.
(27) King, S. M.; Heenan, R. K.; Cloke, V. M.; Washington, C. *Macromolecules* **1997**, *30*, 6215.
(28) Appell, J.; Porte, G.; Rawiso, M. *Langmuir* **1998**, *14*, 4409.
(29) Förster, S.; Burger, C. *Macromolecules* **1998**, *31*, 879.
(30) Pedersen, J. S.; Gerstenberg, M. C. *Macromolecules* **1996**, *29*, 1363.
(31) Pedersen, J. S. *J. Appl. Crystallogr.* **2000**, in press.
(32) Pedersen, J. S. *J. Chem. Phys.*, submitted for publication.
(33) Pedersen, J. S. In *Modern Aspects of Small-angle Scattering*; Brumberger, H., Ed.; Kluwer Academic Press: Norwell, MA, 1995; p 57.
(34) Pedersen, J. S. *Adv. Colloid Interface Sci.* **1997**, *70*, 171.
(35) Guinier, A.; Fournet, G. *Small Angle Scattering of X-rays*; Wiley: New York, 1955.
(36) Fournet, G. *Bull. Soc. Fr. Minéral. Crist.* **1951**, *74*, 39.
(37) Hammouda, B. *J. Polym. Sci., Polym. Phys. Ed.* **1992**, *30*, 1387.
(38) Ashcroft, N. W.; Lekner, J. *Phys. Rev.* **1966**, *83*, 145.
(39) Kinning, D. J.; Thomas, E. L. *Macromolecules* **1984**, *17*, 1712.
(40) Kotlarchyk, M.; Chen, S.-H. *J. Chem. Phys.* **1983**, *79*, 2461.
(41) Pedersen, J. S.; Posselt, D.; Mortensen, K. *J. Appl. Crystallogr.* **1990**, *23*, 321.
(42) Bevington, B. R. *Data reduction and error analysis for the physical sciences*; McGraw-Hill: New York, 1969.
(43) *Polymer Handbook*; Brandrup, J., Immergut, E. H., Eds.; Wiley-Interscience: New York, 1975.
(44) Pedersen, J. S.; Schurtenberger, P. *Macromolecules* **1996**, *29*, 7602.
(45) Halperin, A.; Tirrell, M.; Lodge, T. P. *Adv. Polym. Sci.* **1992**, *100*, 33.
(46) Tao, H.; Huang, C.; Lodge, T. P. *Macromolecules* **1999**, *32*, 1212.
(47) Brown, W.; Nicolai, T. *Colloid. Polym. Sci.* **1990**, *268*, 977.
(48) Pedersen, J. S. Manuscript in preparation.
(49) Derici, L.; Ledger, S.; Mai, S.-M.; Booth, C.; Hamley, I. W.; Pedersen, J. S. *Phys. Chem. Chem. Phys.* **1999**, *1*, 2773.
(50) Pedersen, J. S. *Curr. Opin. Colloid Interface Sci.* **1999**, *4*, 190.
(51) Pedersen, J. S.; Schurtenberger, P. Unpublished and Europhys. Lett. **1999**, *45*, 666.

MA990740W